A COMPARATIVE STUDY OF SALICYLALDOXIME, CYSTEINE AND BENZOTRIAZOLE AS INHIBITORS FOR THE ACTIVE CHLORIDE-BASED CORROSION OF COPPER AND BRONZE ARTIFACTS

Ahmad N. Abu-Baker, PhD
Yarmouk University, Jordan
Ian D. MacLeod, DSc
Western Australian Maritime Museum, Australia
Robyn Sloggett, PhD
The University of Melbourne, Australia
Russell Taylor, PhD
The Commonwealth Scientific and Industrial Research Organization, Australia

Abstract

This study aimed to investigate the effectiveness of salicylaldoxime and cysteine as potential replacements to benzotriazole, the widely used but environmentally unfriendly and not always effective copper corrosion inhibitor. Coupons of modern copper, 5% tin bronze, and 12% tin bronze samples were corroded using an accelerated electrochemical procedure, which involved anodically polarizing the coupons in a solution of 0.5M NaCl + 0.1M $CuCl_2.2H_2O$. X-ray diffraction analysis of the corrosion products showed the presence of copper (I) chloride (CuCl) on the surfaces of the three reference materials. Tin (IV) oxide (SnO_2) was also detected on the surface of the 12% tin bronze.

The interaction of the corrosion inhibitors with the corrosion products was investigated by visual examination and scanning electron microscopy. Benzotriazole and salicylaldoxime formed a surface adherent and aesthetically acceptable green complexes for the corroded copper and bronze, while cysteine formed grey patches that cover the green corrosion on copper and bronze. Accelerated corrosion in an environmental chamber of high relative humidity and temperature (84% RH and 38°C) showed that salicylaldoxime was the most effective inhibitor for the three reference materials against corrosion in these severe environmental conditions. However, electrochemical impedance spectroscopy's results showed that the

benzotriazole was the most effective inhibitor in chloride solutions, and that the effective of cysteine increases with the increase of tin content in the alloy. It was concluded that salicylaldoxime presented a relevant and effective corrosion inhibitor for most conservation applications on corroded copper and bronze, while cysteine presented an environmentally friendly replacement for benzotriazole to protect uncorroded or previously treated by reduction back to metal artifacts.

Keywords: Copper, tin, bronze, artifact, salicylaldoxime, cysteine, benzotriazole, corrosion inhibitor
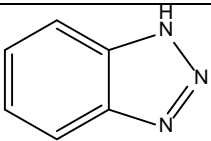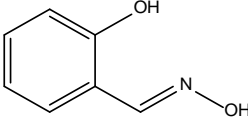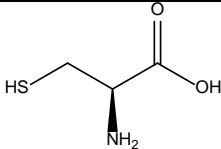
1. Introduction

Conservation treatment of corroded copper-based archaeological artifacts has remained a major concern for conservators and conservation scientists for more than 50 years. Several studies have been conducted to investigate new conservation materials to stabilize these significant cultural materials (Organ 1963; Madsen 1967; Madsen 1971; Angelucci et al. 1978; Ganorkar et al. 1988; Faltermeier 1999; Golfomitsou and Merkel 2004). Corrosion inhibitors are materials which, when added in a small concentration to a corrosive environment, reduce or suppress the corrosion of a metal exposed to that environment (Skerry 1985). Benzotriazole ($C_6H_5N_3$), the main corrosion inhibitor used to stabilize copper based artifacts, was first used in archaeological metal conservation by Madsen (1967) to stabilize bronze disease. This active corrosion resulting from the oxidation of copper (I) chlorides to the powdery basic cupric chlorides, also releases some of the original chloride ions that promote further metal corrosion in a new cycle of the reactions (Scott 1990). Although a number of studies were conducted to test other corrosion inhibitors for copper based artifacts (Angelucci et al. 1978; Merk 1981; Ganorkar et al. 1988; Faltermeier 1999), benzotriazole (BTA) was usually found to be the most effective inhibitor and it remains the most widely used corrosion inhibitor for copper-based artifacts in the conservation field (Mezzi et al. 2012). However, several problems have been identified that relate to the treatment of copper and copper alloys by benzotriazole. Benzotriazole is an environmentally unfriendly, harmful and tumorigenic material (Sigma-Aldrich MSDS 2013), it causes color changes to the treated artifacts and it is not effective at low pH value such as that measured in chloride based corrosion pits of copper artifacts (Scott 1990, Faltermeier 1999). In addition, most previous studies only dealt with copper based artifacts as oxidized copper objects. Only a few studies have considered the corrosion of copper alloying elements and the inhibition of their corrosion. Therefore, investigating new corrosion inhibitors to inhibit the selective dissolution of tin (destanification) or copper (decuprification) in

bronze should be given further attention. The ideal new inhibitor should be safe, effective, easy to apply, environmentally friendly and cause minimal changes in the appearance of the object. Additional advantages accrue if the chemical is relative cheap and is available off the shelf.

Salicylaldoxime ($C_7H_6O_2N$) is a chelating agent that has been used in the solvent extraction, and gravimetric and conductimetric determination of copper (Ramesh et al. 1998; Sarkar 1991). Salicylaldoxime can work as a copper-specific collector, as copper is the only metal that forms a precipitate with salicylaldoxime at pH below 3 (Szymanowski 1993). Cicileo et al. (1999) tested this ligand as a corrosion inhibitor for copper in neutral NaCl solution. They found that it formed a complex with copper (II) ions and precipitated as a yellow-greenish amorphous layer on the copper samples, forming a physical barrier that retarded the attack of corrosive agents. Lamaka et al. (2007) investigated the corrosion inhibiting effect of salicylaldoxime on the aluminium alloy 2042 in neutral chloride solutions. They found that it formed a thin insoluble organic layer on the alloy surface, which inhibited the dissolution of Al and its alloying elements (Cu and Mg). The reaction mechanism, the color of the resulted insoluble complex, and the ability to form a complex at low pH, where BTA usually fails, make this chelating agent a potentially relevant and effective corrosion inhibitor for reactions that produce the characteristic blue-green chloride-based copper corrosion products on the artifacts' surface.

Cysteine is an amino acid that has been investigated as a corrosion inhibitor for copper (Zhang et al. 2005; Ismail 2007; Barouni et al. 2008) and tin (Quraishi et al. 2004). Zhang et al. (2005) found that cysteine inhibited the anodic dissolution of copper in acidic medium more effectively than benzotriazole. Ismail (2007) used electrochemical methods to study the efficiency of cysteine as a non-toxic corrosion inhibitor for copper in chlorinated neutral and acidic media. They found that cysteine inhibited the cathodic reaction to a high extent by adsorption of the amino acid molecules and forming a layer that retarded the transfer of oxygen molecules to the cathodic site on the copper surface. Barouni et al. (2008) examined the corrosion inhibition effectiveness of five amino acids (valine, glycine, arginine, lysine, and cysteine) on copper corrosion in acidic media. Weight loss and electrochemical polarization measurement showed that cysteine was the most effective corrosion inhibitor. The authors attributed that to the presence of the thiol group –SH which was a stronger electron donating group than the functional groups of the other amino acids. Quraishi et al. (2004) mentioned that the amino acid exists in acidic solution as a zwitter ion (a solution species with both a positive or cationic and a negative or anionic ionic charges on the molecule). The cationic part of this ion adsorbs on the cathodic sites of tin and decreases the cathodic reaction, while the

anionic part adsorbs on the anodic sites and decreases the anodic dissolution of tin. As cysteine showed inhibitive effect on the corrosion of copper and tin, it was proposed to be investigated in this study as the previous results indicate that it is likely to have good inhibition for the corrosion of copper and bronze.

Table 1: The chemical structures of the corrosion inhibitors	
Benzotriazole (BTA) ($C_6H_5N_3$)	
Salicylaldoxime ($C_7H_7NO_2$)	
Cysteine ($C_3H_7NO_2S$)	

This study investigated the surface morphological changes of corroded copper and bronze reference coupons when treated with benzotriazole, salicylaldoxime and cysteine (Table 1). The use of copper and two tin bronze reference alloys, 5% tin bronze, and 12% tin bronze, as the reference materials for the accelerated corrosion and testing of new corrosion inhibitors, was based on previous experience with the behavior of α-phase tin archaeological bronzes that showed a similar range of compositions (Abu-Baker 2008). The range of compositions facilitated the study of the effect of the amount of tin in the alloy on the corrosion type and products that can form, and comparison of the effect of corrosion inhibitors on copper and its alloying elements. X-ray diffraction (XRD) was used to characterize the corrosion products. Visual examination and scanning electron microscopy (SEM) were used to investigate the surface morphological changes as a result of binding of the corroded copper and bronze coupons when treated with the three corrosion inhibitors. The study also aimed to compare the efficiency of salicylaldoxime, cysteine and benzotriazole (BTA) on the reference coupons by exposure in a chamber of relatively high humidity and temperature (84% RH, 38°C) and electrochemical impedance spectroscopy (EIS).

2. Experimental procedure

2.1. The reference materials pretreatment (anodic polarization followed by inhibitors application) and characterization (SEM and XRD)

Sheets of the reference copper and 5% tin bronze were bought from the supplier AMAC alloys. The compositions of these materials as provided by the suppliers are:

- High conductivity copper-110: 99.95% Cu, 0.02% O
- Wrought phosphorous bronze-510: 94.97% Cu, 5.00% Sn, 0.03% P

The 12% tin bronze was not commercially available and was prepared by alloying a mixture of copper (pieces from the copper-110 used in this research) with tin pieces in a weight percent of 88% Cu:12% Sn. The alloy was prepared by direct addition of tin to molten copper in a crucible. A sample of the resultant alloy was analyzed by electron microprobe elemental analysis, which was performed on a Cameca SX50 electron microprobe. The weight percent of copper and tin in the resultant alloys was about 88% Cu:12% Sn. Experimental details of the preparation and analysis of this alloy are described in Abu-Baker (2009).

Figure 1: A drawing representing the set-up of the anodic polarization process
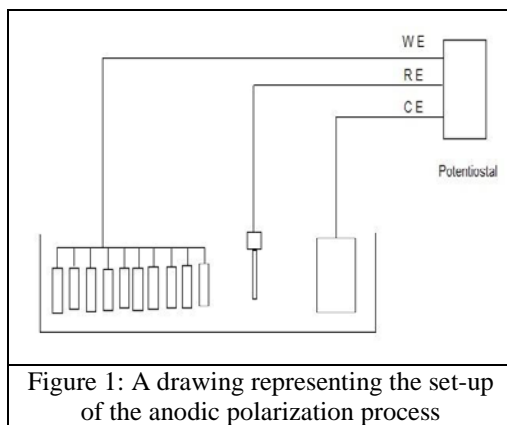
Coupons of the reference copper (7.5x2.5x0.12 cm), 5% tin bronze (7.5 x 2.5 x 0.16 cm), and 12% tin bronze (4.0 x 3.0 x 0.1 cm) were polished with 600, 800, 1000, and 1200 silicon carbide papers and degreased in acetone in an ultrasonic bath for two minutes. The synthetic corrosion layers were formed electrochemically. For each of the types of copper and copper alloy reference materials, an electrochemical cell was formed of ten coupons (working electrode WE), copper sheet of an area similar to that of the working electrode (counter electrode CE) and an Ag/AgCl/sat'd KCl reference electrode (RE). The three electrodes were connected to a Pine Instruments bipotentiostat model AFCBPI. The ten coupons formed a single working electrode by connecting them together using a bare copper wire that was attached to each coupon using a plastic peg (Figure 1). The

electrochemical cell was setup in a Perspex box that was filled with about 2 liters of the corrosive electrolyte (0.5M NaCl + 0.1M $CuCl_2$) for copper and the 5% tin bronze coupons, while the volume of the electrolyte for the smaller tin bronze samples was about 1 liter. The coupons were corroded for three days at a low anodic potential (i.e. 100mV vs. Ag/AgCl) to gradually form a uniform corrosion layer, then in a second stage the potential was raised to 200mV vs. Ag/AgCl for one day to increase the thickness of the corrosion layer. The coupons were then rinsed with deionized water, dehydrated with acetone, and finally dried in the oven at $50^{o}C$ for 30 minutes for the initial drying and development of the corrosion layer. This was followed by heating at $105^{o}C$ for 30 minutes for the complete evaporation of any water residues. The set-up of this experiment produced 10 corroded coupons of each reference material, which were sufficient for XRD analysis samples and replicates for the environmental chamber evaluation experiment of each of the corrosion inhibitors.

SEM was used to study the surface of the coupons after the accelerated corrosion process and treatment with the corrosion inhibitors. The SEM analysis was carried out on the surface of the corroded coupons using an FEI Model XL30 ESEM. Wet mode was used at 0.5 Torr H_2O and the operating conditions for the electron beam were 20kV and spot size 4–6. The corrosion products were investigated and characterized by XRD. The corrosion products were scratched off from the surfaces of the corroded reference materials, ground and analyzed by a Philips PW1800 powder X-ray diffraction instrument. Copper Kα radiation (λ=1.5418 Å) was used for the analysis and the spectra were acquired at 40 kV, 30 mA and a step size of 0.05^{o} in 2θ. The assignment of the minerals was based on the database of the Joint Committee Powder Diffraction Standards-International Centre for Diffraction Data (JCPDS-ICDD).

2.2. Evaluation of the inhibition
2.2.1. Environmental chamber
Coupons of the synthetically corroded copper and bronzes were treated with the corrosion inhibitors' solutions by immersion for 24 hours in 100 ml of 0.01M concentration in ethanol at ambient temperature. The basic methodology used is that found in the ASTM D2247–02 and ASTM D1735–04 procedures, which describe the techniques for testing the water resistance of coatings in an enclosed chamber with 100% relative humidity and at $38^{o}C$. These procedures were adapted to the test the effectiveness of the corrosion inhibitors on the samples of this study by modifying the parameters; decreasing the relative humidity of the test to 84% relative humidity since this is a more realistic value experienced in poor storage conditions. This

relative humidity was obtained using a saturated solution of potassium chloride to minimize the effect of water condensation on the samples.

Figure 2: The set-up of the coupons in the desiccator for the high relative humidity and temperature experiment

The chamber for the humidity and temperature experiment was a desiccator (300 mm in diameter) equipped with a 100 ml beaker containing a saturated solution of potassium chloride at the bottom. This provides a relative humidity of about 84% at 38°C (Rockland 1960). The coupons were placed vertically on small plastic supports on a perforated porcelain plate in the middle of the desiccator (Figure 2), and the desiccator was tightly closed and kept in the oven (Gualtex Solid Stat model OG2452) set on 38°C for the entire duration of the experiment. Duplicate samples of each inhibitor on each reference material were tested. The experiment was stopped after 72 hours as various corrosion signs appeared on most of the coupons. The decision was made to stop the experiment at this stage since it enabled assessment of the differential effectiveness of the inhibitors. If the coupons were left for a longer time, further corrosion would have occurred on all samples to such an extent that comparative analysis would not be able to be fully evaluated. The samples were evaluated by visual and microscopic examination. The microscopic examination was done using an Olympus BX51 polarized light microscope. Photomicrographs were taken using an Olympus DP70 camera attachment.

2.2.2. EIS

Un-corroded coupons of copper and the two bronzes were used as the working electrodes for the EIS measurements. The coupons were polished with 600, 800, 1000, and 1200 silicon carbide papers, and then polished with diamond paste beginning at 8–4 μm and reducing down to a highly polished surface using a 0.5 μm paste. They were washed with distilled water, degreased in acetone in an ultrasonic bath for two minutes, and finally rinsed with distilled water and dried in the oven. The impedance measurements were carried out in a cylindrical Perspex cell that contained a solution of

0.1M NaCl and 0.01M of each of the corrosion inhibitors. The reference electrode was an Ag/AgCl/sat'd KCl and a platinum wire electrode was used as the counter electrode. The exposed area of the working electrode to the corrosive solution was 1.0 cm^2 which had been determined by careful masking of the surface. The electrochemical cell was set in a Faraday cage and the impedance was then measured using AC signals of amplitude equals 5mV peak to peak at the open circuit potential in the frequency between 10 kHz and 10 mHz. An EG&G electrochemical impedance analyzer-model 6310 was used for the experiment. Duplicate samples of each inhibitor on each reference material were tested. Impedance results were analyzed using Zview 3.1c software application.

3. Results and discussion
3.1 Characterization of the coupons after anodic polarization and application of the inhibitors

The pre-treatment of the coupons in order to simulate corroded archaeological artifacts was adapted from the procedure of Casaletto et al. (2006). The same corrosive solution of 0.5M NaCl + 0.1M CuCl$_2$.2H$_2$O was used. However, the procedure employed was different. Casaletto et al. sprayed their reference alloys with the corrosive solution and exposed them to a 100% RH at 30°C for 15 day. In this experiment, however, the coupons were immersed in that solution, and an external potential was applied to accelerate the corrosion process and anodically polarize both the internal alloy in addition to the outer surface.

Figures 3–5 show representative copper and bronze coupons after the accelerated corrosion process and application of the three inhibitors. Copper coupons were covered with a pale-green corrosion layer. 5% tin bronze coupons were also covered with a green corrosion layer, which were mixed with small patches of a pale-yellow corrosion product. The amount of the pale-yellow corrosion product was higher for the 12% tin bronze. The treatment of the corroded reference coupons with the inhibitors' solutions made changes to the morphology and color of the corrosion layer. The visual appearance of the treated coupons is a major concern in the conservation field of archaeological artifacts as it has a great effect on the historic and aesthetic values of the artifact if the color changes are irreversible. Some corrosion inhibitors show a high effectiveness when evaluated by electrochemical or surface analytical techniques; however they are unsuitable for conservation purposes if they disfigure the historic appearance of the artifact. As the figures show, the BTA treated coupons show darkening in the green color of the corrosion layer of the copper, 5% tin bronze, and 12% tin bronze coupons. The salicylaldoxime treated coupons show that the green corrosion layer of the copper, 5% tin bronze, and 12% tin bronze coupons

became darker, porous and glossy. This preliminary assessment shows that visual changes caused by salicylaldoxime are relatively acceptable and the result of treatment is an insoluble, adherent and color relevant inhibited corrosion layer. The cysteine treated coupons show grey patches that cover the green corrosion on copper, 5% tin bronze and 12% tin bronze coupons, which make a change of the original color of the corrosion products.

Figure 3: From left, corroded copper without inhibitor, corroded and treated with BTA, salicylaldoxime and cysteine

Figure 4: From left, corroded 5% tin bronze without inhibitor, corroded and treated with BTA, salicylaldoxime, and cysteine

Figure 5: From left, corroded 12% tin bronze without inhibitor, corroded and treated with BTA, salicylaldoxime, and cysteine

The effect of each of the tested inhibitors on the three reference materials coupons was investigated by SEM. Table 2 shows the SEM images of the corroded reference coupons untreated and treated with three corrosion inhibitors. The SEM images in the table show that BTA forms a film that follows the morphology and crystal formation for copper and the two bronzes. The SEM images of salicylaldoxime treated corroded coupons show that this inhibitor is working as a chelating agent and it does not form a film

that follows the morphology of the corrosion product crystals. The molecules of this inhibitor anchor on the surface of the corroded samples and form a discrete layer. The SEM images of cysteine treated coupons show that cysteine forms a layer that covers the crystals of the corrosion products on copper and the 5% tin bronze and less uniformly on the 12% tin bronze.

Table 2: SEM images of corroded reference materials without inhibitor, corroded and treated with BTA, salicylaldoxime and cysteine			
	Copper	5% tin bronze	12% tin bronze
Corroded surface without inhibitor			
BTA inhibited			
Salicylald oxime inhibited			
Cysteine inhibited			

The XRD characterization of the corrosion products on the corroded coupons shows that nantokite (copper (I) chloride CuCl) is the main corrosion product on the surface of copper coupons (Figure 6).
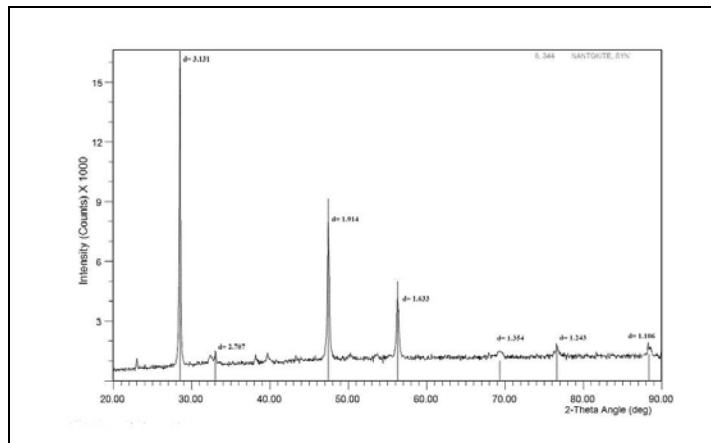
Figure 6: XRD spectrum of the corrosion on the copper
coupons with nantokite being the main corrosion product

Nantokite was also detected as the main corrosion of the 5% tin bronze (Figure 7). No tin-related corrosion products were detected by XRD. This can be ascribed to the fact that there was only a very small amount of the pale-yellow corrosion (that can be related to tin) on the surface and that was not detected by the XRD.
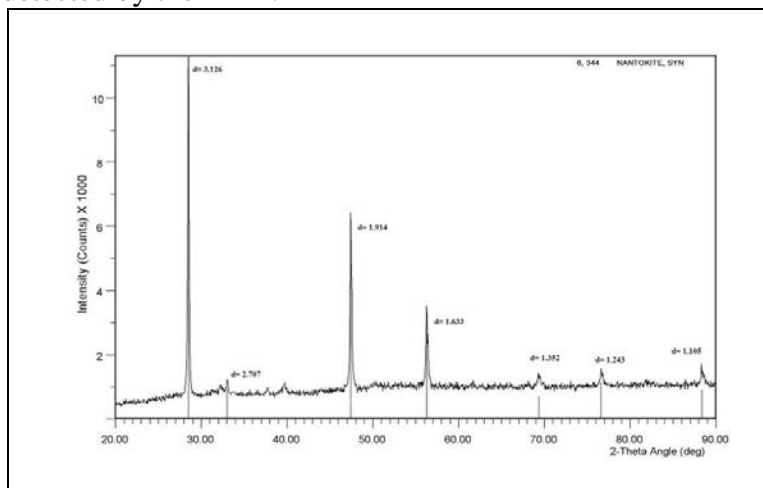

Figure 7: XRD spectrum of the corrosion on the 5% tin bronze
coupons with nantokite being the main corrosion product

For the 12% tin bronze, tin (IV) oxide (SnO_2) was detected in the XRD analysis in addition to nantokite and this can be ascribed to the substantial amount of the pale-yellow corrosion on the surface of the coupons (Figure 8).
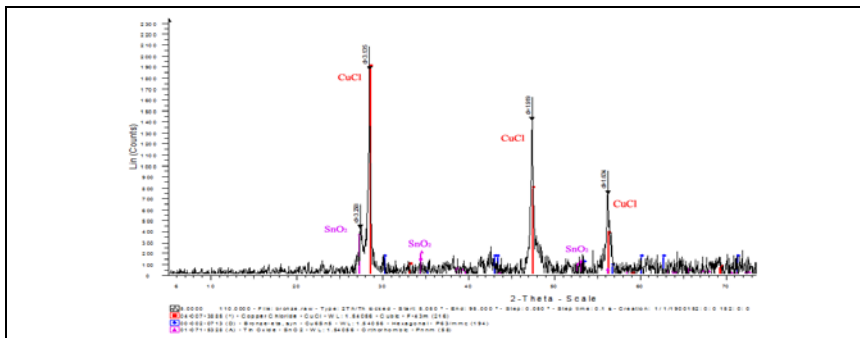
Figure 8: XRD spectrum of the corrosion on the 12% tin bronze coupons with nantokite (CuCl) and tin (IV) oxide (SnO$_2$) being the main corrosion products

3.2. Evaluation of the inhibition
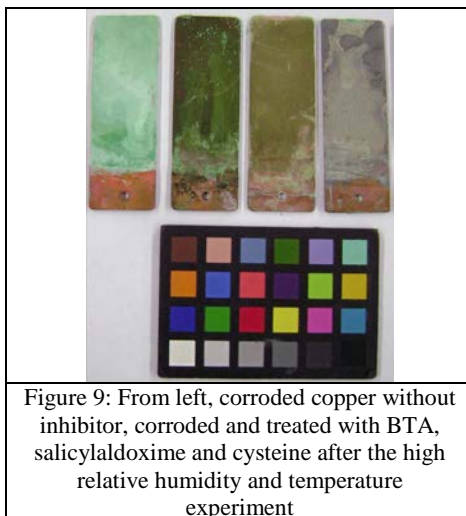## 3.2.1. Environmental chamber

Figure 9: From left, corroded copper without inhibitor, corroded and treated with BTA, salicylaldoxime and cysteine after the high relative humidity and temperature experiment

The photographic data for copper coupons after the experiment are shown in Figure 9. When compared with the status of the coupons before the experiment as appeared in Figure 3, it can be observed that the coupons had variable degrees of corrosion during the experiment. Photographic data for each coupon before and after the experiment combined with observations from the microscopic images of the coupons after the experiment in Table 3 show that the un-inhibited coupon became completely covered with a pale blue-green corrosion layer during the corrosion test and the microscopic examination shows this as a uniform corrosion layer covering the whole surface. The BTA treated coupon was not corroded in the same uniform manner which demonstrated that the BTA provided some protection against the corrosive environmental conditions. However, that protection was not sufficient to prevent corrosion where a number of blisters started to appear

239

on the surface. These blisters formed active corrosion sites that could lead to further corrosion. Salicylaldoxime showed the best protection in this experiment where no active corrosion blisters appeared on the surface of the copper coupon. The cysteine treated coupon had a few isolated corrosion spots as seen in the microscopic image.
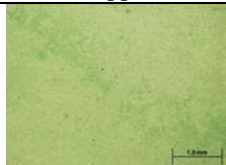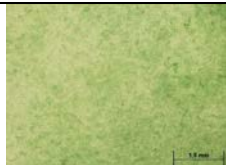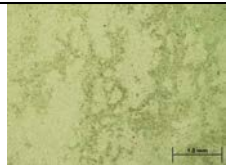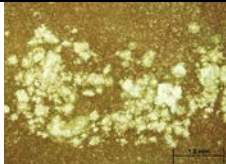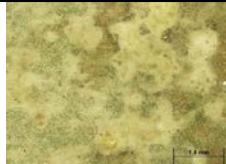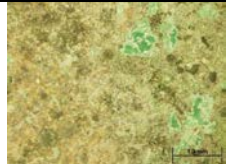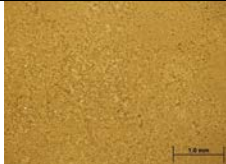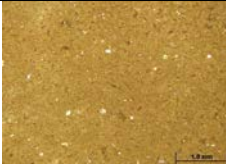

Figure 10: From left, corroded 5% tin bronze without inhibitor, corroded and treated with BTA, salicylaldoxime and cysteine after the high relative humidity and temperature experiment

Figure 10 shows each of the 5% tin bronze coupons after the experiment. Perusal of the photographic and microscopic data in Figures 4 and 10 and Table 3 confirms that behavior of the 5% tin bronzes is similar to the copper coupons where th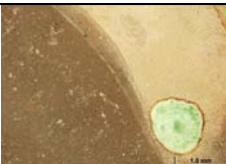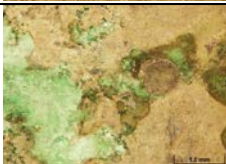e corrosion layer on the un-inhibited corroded coupon was completely converted to a pale blue-green uniform corrosion layer covering the whole surface. The BTA treated coupon had corrosion blisters and some areas around them have started to flake off. The salicylaldoxime treated coupon had the least change with no noticeable corrosion spots or blisters on the surface. The cysteine treated coupon had an increase in the coupon darkness, that is a loss of hue in the $L^*a^*b^*$ system, and some major pale blue-green corrosion spots and the corrosion pattern appeared to follow a dendritic pattern indicating that the copper-rich α-phase has been attacked.

Figure 11: From left, corroded 12% tin bronze without inhibitor, corroded and treated with BTA, salicylaldoxime, and cysteine after the high humidity and temperature experiment

In a similar vein Figure 11 shows each of the 12% tin bronze coupons after the experiment. As can be discerned from the Figures 5 and 11 and from the images in Table 3, the un-inhibited corrosion coupon formed a pale blue-green corrosion product on the whole surface. The BTA treated coupon had some corrosion spots scattered over the surface which indicated that there was some form of localized corrosion. The salicylaldoxime inhibited coupon had a few corrosion spots near the edge, while about one third of the cysteine treated coupon was covered by the pale blue-green corrosion product.

Table 3: Microscopic images of the coupons after the high relative humidity and temperature experiment			
	Copper	5% tin bronze	12% tin bronze
Uninhibited			
BTA inhibited			
Salicylaldoxime inhibited			
Cysteine inhibited			

It was observed that the copper and two bronzes coupons tested in this experiment had predominately copper corrosion products formed on the surface as a result of being subject to humidity and temperature in the experimental regime. No tin corrosion products emerged on the surface as the experimental conditions do not facilitate mobilization of tin corrosion products. This is because the SnO_2 detected by XRD seems to remain as a primary corrosion layer underneath the secondary copper mineralization. The lack of any $Sn^{(II)}$ corrosion products is due to the well oxygenated micro-environment of the corrosion experiment with two rapid two-electron steps and concomitant hydrolysis that resulted in the formation of SnO_2 (MacLeod and Wozniak 1997). It seems that the tin (IV) oxide remained enriched at the

241

bottom of the corrosion products layer, while the more soluble copper corrosion products migrated to the periphery as outgrowth corrosion. However, the presence of tin in the two bronzes affected their performance against the accelerated corrosion by high humidity and temperature in comparison with copper. It is known that alloying copper with tin enhances the corrosion resistance in the resulting alloy, and that can be attributed to a formation of an insoluble tin (IV) oxide ($SnO_2.xH_2O$) protective barrier against mild corrosive conditions (Strandberg et al. 1997). However, for samples which are already pre-corroded, such as the ones of this study, the investigation aimed to assess the durability of corrosion inhibitors and their protection against further corrosion. Although tin corrosion products are protective, the presence of different corrosion products on the surface of the samples hindered a formation of a complete and uniform inhibitor film on the surface. The amount of surface coverage of corrosion outgrowth on the bronzes after the high humidity and temperature experiment is higher than that of copper coupons. This finding could be attributed to the emergence of the new copper hydroxyl-chloride corrosion products over the tin corrosion products that stay enriched underneath it, closer to the metal surface. The presence of these corrosion products will improve access of oxygen to the parent alloy surface and so promote pitting corrosion reactions.

3.2.2. EIS

Figures 12–14 show representative Bode magnitude plots of the impedance spectra of the un-corroded three reference materials, with and without the corrosion inhibitors in the 0.1M NaCl corrosive electrolyte. The results show that impedance modulus varies not only from one inhibitor to another, but also from one alloy to another for the same inhibitor. This suggests that the efficiency of the inhibitor is affected by the amount of copper alloying element that affects the corrosion mechanism and the complex formation with the corrosion inhibitor.

Figure 12: Bode magnitude plots of impedance spectra of copper in 0.1M NaCl with and without the tested corrosion inhibitors

242
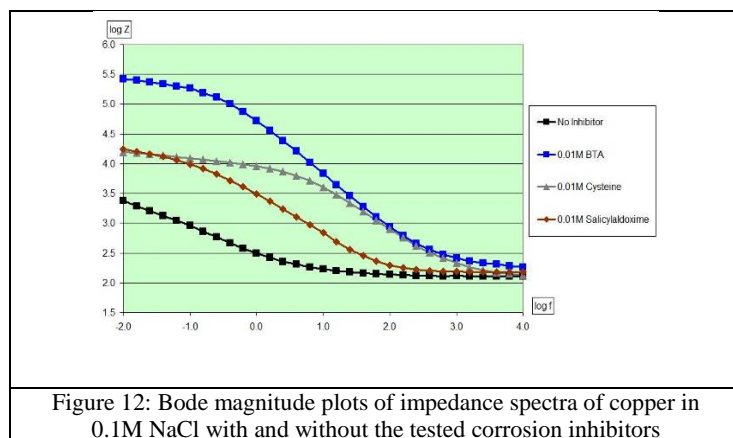
The Bode magnitude plots of impedance spectra for copper samples in Figure 12 show that BTA is the most effective corrosion inhibitor as its impedance modulus low frequency end is about two decades higher than that of copper without inhibitor. The other two corrosion inhibitors slightly vary in their low-frequency modulus end which does not exceed one decade higher than that of copper without inhibitor, which is half of the impedance increase caused by BTA.
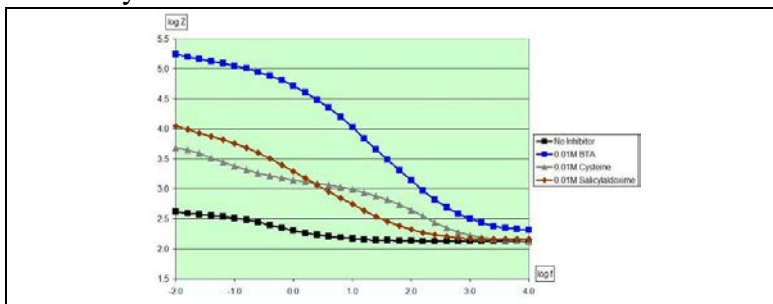

Figure 13: Bode magnitude plots of impedance spectra of 5% tin bronze in 0.1M NaCl with and without the tested corrosion inhibitors
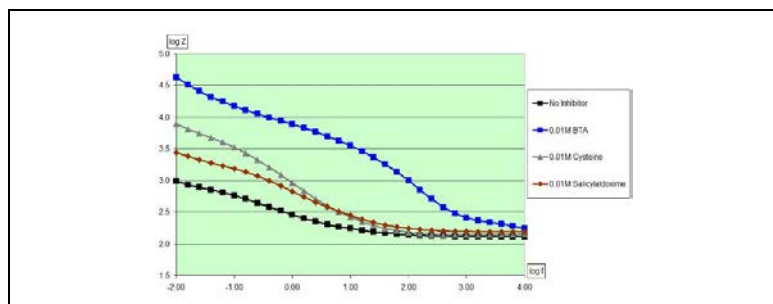
Figure 14: Bode magnitude plots of impedance spectra of 12% tin bronze in 0.1M NaCl with and without the tested corrosion inhibitors

For the 5% tin bronze, Figure 13 shows that BTA has the highest impedance modulus at low frequency which is about three decades higher than that of the un-inhibited sample. It is then followed by salicyladoxime and finally cysteine.

The 12% tin bronze impedance moduli in Figure 14 show that BTA has the highest low frequency end. The other two inhibitors have a lower effect on the low frequency end, where cysteine comes in the second place followed by salicylaldoxime.

The increase of tin percentage in the alloy decreases the $\log_{10}|impedance|$ value, therefore the corrosion resistance, of the inhibitors at low frequency. For example, 0.01M BTA registers 5.4 on copper and 5.2 on 5% tin bronze while it is just 4.6 on 12% tin bronze, and this could be a

result of the difference in the reactivity of copper and tin with the corrosion inhibitor, which leads to less uniform corrosion inhibitor film on the surface with the increase of tin content in the alloy.

To obtain quantitative data from EIS measurements, the system under investigation should be modeled on an equivalent circuit in which each element models specific function of the sample (Loveday et al. 2004). A simple corrosion system of uniform corrosion and mass-transfer controlled corrosion reaction can be represented by the simple equivalent circuit (Figure 15):
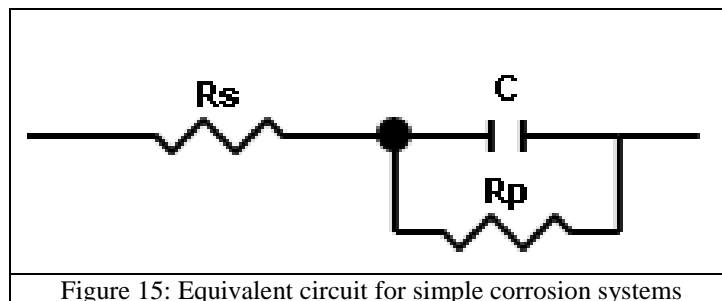

Figure 15: Equivalent circuit for simple corrosion systems

where C is the double layer capacitance, R_s is the solution resistance that also contains all ohmic resistances in the system, while R_p is the polarization resistance.

Several modifications could be made on the basic equivalent circuit according to the conditions of the system under investigation. For example, additional elements can be added to the equivalent circuit to make the experimental data fit better (Mansfeld 2006, pp. 466–468). The elements of an appropriate equivalent circuit can be determined according to what processes are happening on the surface of the tested sample. In the case of impedance controlled by diffusion, an additional resistive element should be added to the simple equivalent circuit in Figure 15 in series with the R_p. This element is called the Warburg impedance (W) and evidenced by a straight line, at higher frequencies, at 45° in the Nyquist plot (Jones 1992, p. 109). This was the case of most of the impedance results of the tested samples (Nyquist plots are not presented in this article). In addition, for a better fit of the impedance spectra, the double layer capacitance (C) should be replaced by a constant phase element (CPE) modeling non-ideal capacitive behavior. Constant phase element (CPE) defines the capacitive properties of the film and two values, CPE-T and CPE-P, define the properties of the CPE. CPE-P gives the phase angle of CPE (if CPE-P=1 then CPE is a simple capacitor, if CPE diverges from 1 then the film is uneven), and CPE-T represents the mean capacitance of the film and is proportional to the mean thickness of the film. Based on that, the circuit in Figure 16 was found to be suitable to be a general equivalent circuit for the results. Using this circuit, impedance

parameters were calculated by the Zview software (fitting plots are not presented in this article). In some cases there was a slight deviation from ideal fit on this circuit as a result of the differences in the chemistry of inhibitors and their interaction with the three reference materials. The circuit was, however, used to fit all results of copper and the two bronzes so that the calculations are based on the same equivalent circuit.
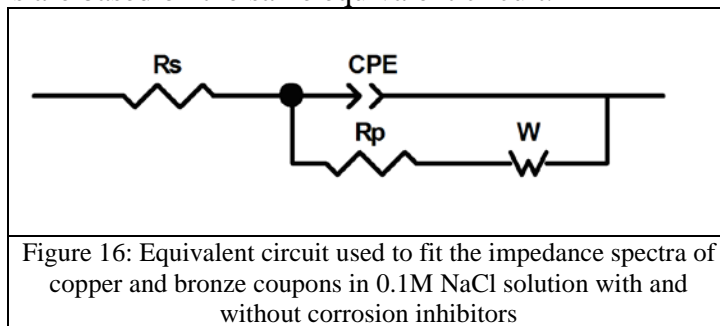

Figure 16: Equivalent circuit used to fit the impedance spectra of copper and bronze coupons in 0.1M NaCl solution with and without corrosion inhibitors

Table 4–6 show impedance parameters of the un-inhibited and inhibited copper and bronze samples arranged according to the inhibition efficiency (IE) calculated by the formula:

$$IE\% = \frac{R_p - R_p^o}{R_p} \times 100\%$$

where R_p and R_p^o are the polarization resistances of the inhibited and un-inhibited solutions, respectively. Increased values of R_p are indications of the increase of surface coverage (θ) that can be given by the formula (Ehteshamzadeh et al. 2006a, 2006b):

$$(1 - \theta) = \frac{R_p^o}{R_p}$$

As Table 4 shows, for copper, the order of the tested inhibitors from high to low IE is:
0.01M BTA> 0.01M cysteine> 0.01M salicylaldoxime.

Inhibitor	R_s (Ω cm^2)	CPE-T (F cm^{-2})	CPE-P	R_p (Ω cm^2)	W (Ω s$^{0.5}$)	IE %
No inhibitor	1.3E+02	1.4E-03	6.1E-01	3.2E+03	3.6E+03	
0.01M BTA	2.0E+02	3.5E-06	9.0E-01	2.1E+05	4.8E+04	98.5
0.01M Cysteine	1.3E+02	8.1E-06	7.9E-01	1.0E+04	5.3E+03	68.7
0.01M Salicylaldoxime	1.5E+02	6.4E-05	7.8E-01	9.0E+03	7.0E+03	64.2

Table 4: Impedance parameters for copper in 0.1M NaCl with and without corrosion inhibitors

Table 5 shows impedance parameters of the un-inhibited and inhibited 5% tin bronze samples arranged according to the inhibition

efficiency (IE). The order of the tested inhibitors from high to low IE is: 0.01M BTA> 0.01M salicylaldoxime> 0.01M cysteine.

	R_s (Ω cm^2)	CPE-T (F cm^{-2})	CPE-P	R_p (Ω cm^2)	W (Ω s$^{0.5}$)	IE %
Table 5: Impedance parameters for 5% tin bronze in 0.1M NaCl with and without corrosion inhibitors						
Inhibitor						
No inhibitor	1.3E+02	2.7E-03	6.3E-01	1.1E+02	1.7E+02	
0.01M BTA	2.1E+02	2.6E-06	8.8E-01	8.8E+04	7.4E+04	99.9
0.01M Salicylaldoxime	1.4E+02	1.5E-04	6.5E-01	1.0E+04	3.7E+02	98.9
0.01M Cysteine	1.3E+02	1.8E-05	7.6E-01	9.9E+02	5.4E+03	88.7

Table 6 shows impedance parameters of the un-inhibited and inhibited 12% tin bronze samples arranged according to the inhibition efficiency (IE). The order of the tested inhibitors from high to low IE is: 0.01M BTA> 0.01M cysteine> 0.01M salicylaldoxime.

Inhibitor	R_s (Ω cm^2)	CPE-T (F cm^{-2})	CPE-P	R_p (Ω cm^2)	W (Ω s$^{0.5}$)	IE %
Table 6: Impedance parameters for un-corroded 12% tin bronze with and without corrosion inhibitors in 0.1M NaCl						
No inhibitor	1.3E+02	1.6E-03	5.7E-01	8.0E+02	8.9E+02	
0.01M BTA	1.7E+02	7.6E-06	7.7E-01	6.5E+03	2.2E+04	87.7
0.01M Cysteine	1.4E+02	3.0E-04	7.2E-01	6.3E+03	1.3E+03	87.3
0.01M Salicylaldoxime	1.5E+02	4.9E-04	6.1E-01	2.1E+03	1.0E+03	62.1

As the Tables 4–6 show, BTA is most effective on copper and 5% tin bronze followed by the 12% tin bronze. The inhibition of BTA can be related to the formation of $Cu^{(I)}BTA$ and $Cu^{(II)}BTA$ polymeric complexes (Sease 1978; Brostoff 1997; Golfomitsou and Merkel 2007). Tin also forms a complex with BTA, $Sn^{(IV)}(BTA)_2$ (Molodkin 1997). The formation of polymeric films for copper with BTA can interpret the higher efficiency on copper in comparison with that on 12% tin bronze where tin does not form such polymeric films.

Cysteine has the highest IE% on the two bronzes followed by that of copper. Cysteine bonds to $Cu^{(I)}$ and $Cu^{(II)}$ through its thiol S atom (Llopiz et al. 1979) or through both sulfur and nitrogen of the thiol and amino groups (Panigarahi et al. 2006; Ismail 2007; Dokken et al. 2009), while it is a tridentate ligand for tin (Llopiz et al.1979). Thus, in the case of 5% tin bronze and 12% tin bronze the presence of Sn increases the strength of

inhibitor's chemisorption on the surface of the alloy and so increases the corrosion inhibition efficiency.

For salicylaldoxime, the efficiency of the inhibitor on the un-corroded samples is the highest for 5% tin bronze followed by copper and finally the 12% tin bronze. Its inhibition is associated with the formation of $Cu^{(II)}(salox)_2$ complex between the metal ion and the deprotonated phenolic oxygen and the nitrogen atom of the oxime group in the salicylaldoxime molecules (Aggarwal et al. 1984; Ramesh et al.1998). For the 12% tin bronze, the presence of a relatively high tin content decreases the IE% as a result of less homogeneous surface. The presence of different corrosion mechanisms on the surface of this alloy hinders the formation of a complete and uniform inhibitor film on the surface. Although tin corrosion products are protective, the film decays quickly, and so a lower impedance and consequently increasing corrosion rate is achieved with the high increase of tin in the alloy (Brunoro et al. 2003).

4. Conclusion

This study aimed to investigate salicylaldoxime and cysteine as more environmentally friendly corrosion inhibitors to replace benzotriazole as copper and bronze corrosion inhibitors.

The results derived from the experimentation utilizing the accelerated humidity and temperature chamber showed the high degree of effectiveness of salicylaldoxime in the inhibition of the active corrosion of copper and bronze, and in providing resistance to the severe environment corrosion to higher degree than that provided by benzotriazole. The good stability of the corrosion inhibitor complex with the corrosion products of copper and bronze, and the formation of an insoluble surface adherent inhibited corrosion layer with a color that is close to the original color of the chloride based corrosion products, make salicylaldoxime a promising corrosion inhibitor.

The results of EIS showed that benzotriazole had the highest impedance for corrosion in the sodium chloride aqueous solution. The results of cysteine were also interesting, especially for the 12% tin bronze where it had higher impedance than that of it on copper, and the inhibition efficiency was very close to that of benzotriazole. This could indicate an inhibition for the selective corrosion of the alloying element tin. However, the main drawback of cysteine was the color change that it caused on the corroded samples examined in the high relative humidity and temperature experiment.

Based on the result of the two evaluation methods, it can be concluded that salicylaldoxime presents a relevant corrosion inhibitor for most conservation applications that relate to the issues of stabilizing the corrosion of corroded archaeological copper and bronze artifacts in poor

museum or on-site storage conditions, while cysteine presents a relevant inhibitor for the cases in which no color change of the surface will happen, such as on un-corroded or treated by reduction back to metal artifacts, where it forms a protective layer that does not change the surface appearance.

Acknowledgements

References:
Abu-Baker, A. 2008. Investigating the corrosion and microstructure of five copper-based archaeological artefacts from *Tell el-Ajjul*. *AICCM Bulletin*. 31: 87–96.
Abu-Baker, A. 2009. Copper and copper alloys: history, corrosion and corrosion inhibition. Unpublished PhD thesis. The University of Melbourne, Melbourne.
Aggarwal, R. C. Singh, N. K. and Singh, R. P. 1984. Magnetic and spectroscopic studies on salicylaldoxime and o-hydroxynaphthaldoxime complexes of some divalent 3d metal ions. *Synthesis and Reactivity in Inorganic, Metal-Organic, and Nano-Metal Chemistry* 14(5): 637–650.
Angelucci, S. Fiorentino, P. Kosinkova ,J. and Marabelli, M. 1978. Pitting corrosion in copper and copper alloys: comparative treatment tests. *Studies in Conservation* 23(4): 147–156.
ASTM 2004, Standard practice for testing water resistance of coatings using water fog apparatus. D1735–04. Philadelphia: American Society for Testing and Materials.
ASTM 2002, Standard practice for testing water resistance of coatings in 100% relative humidity. D2247–02. Philadelphia: American Society for Testing and Materials.
Barouni, K. Bazzi, L. Salghi, R Mihit, M. Hammouti, B. Albourine, A. El Issami, S. 2008. Some amino acids as corrosion inhibitors for copper in nitric acid solution. *Materials Letters*, vol. 62(19): 3325–3327.
Brostoff, L. 1997. Investigation into the interaction of benzotriazole with copper corrosion minerals and surfaces. In *Metal 95: Proceeding of the*

International Conference on Metals Conservation, ed. I. MacLeod et al. London: James and James. 99–108.

Brunoro, G. Frignani, A. Colledan, A. and Chiavari, C. 2003. Organic films for protection of copper and bronze against acid rain corrosion. *Corrosion Science* 45(10): 2219–2231.

Casaletto, M. P. Caruso, F. De Caro, T. Ingo, G. M. and Riccucci, C. 2007. A Novel scientific approach to the conservation of archaeological copper alloys artefacts. In *Metal 07: proceedings of the International Conference on Metals Conservation, Book 2*, ed. C. Degrigny et al. Amsterdam: Rijksmuseum. 20–25.

Casaletto, M. P. De Caro, T. Ingo, G. M. and Riccucci, C. 2006. Production of reference "ancient" Cu-based alloys and their accelerated degradation methods. *Applied Physics A* 83(4): 617–622.

Cecile, J. Cruz, M. Barbery, G. and Fripiat, J. 1981. Infrared spectral study of species formed on malachite surface by adsorption from aqueous salicylaldoxime solution. *Journal of Colloid and Interface Science* 80(2): 589–597.

Cicileo, G. P. Rosales, B. M. Varela, F. E. and Vilche, J. R. 1999. Comparative study of organic inhibitors of copper corrosion. *Corrosion Science* 41(7): 1359–1375.

Dokken, K. Parsons, J. McClure, J. and Gardea-Torresdey, J. 2009. Synthesis and structural analysis of copper(II) cysteine complexes. *Inorganica Chimica Acta* 362(2): 395–401.

Ehteshamzadeh, M. Shahrabi, T. and Hosseini, M. 2006a. Inhibition of copper corrosion by self-assembled films of new Schiff bases and their modification with alkanethiols in aqueous medium. *Applied Surface Science* 252(8): 2949–2959.

Ehteshamzadeh, M. Shahrabi, T. and Hosseini, M. 2006b. Innovation in acid pickling treatment of copper by characterization of a new series of Schiff Bases as corrosion inhibitors. *Anti-Corrosion Methods and materials* 53(5): 296–302.

Faltermeier, R. B. 1999. A corrosion inhibitor test for copper-based artifacts. *Studies in Conservation* 44(2): 121–128.

Ganorkar, M. C. Rao, V. P. Gayathri P. and Rao, T. A. S. 1988. A novel method for conservation of copper-based artifacts. *Studies in Conservation* 33(2): 97–101.

Golfomitsou, S. and Merkel, J. F. 2004. Synergistic effects of corrosion inhibitors for copper and copper alloy archaeological artefacts. In *Metal 04: Proceeding of the International Conference on Metals Conservation*, ed. J. Ashton and D. Hallam. Canberra: National Museum of Australia. 344–368.

Golfomitsou, S. and Merkel, J. F. 2007. Understanding the efficiency of combined inhibitors for the treatment of corroded copper artefacts. In *Metal*

07: proceedings of the International Conference on Metals Conservation, Book 5, ed. C. Degrigny et al. Amsterdam: Rijksmuseum. 38–43.

Jones, D. 1992. *Principles and pevention of crrosion*. New York: Macmillan Publishing Company.

Ismail, K. 2007. Evaluation of cysteine as environmentally friendly corrosion inhibitor for copper in neutral and acidic chloride solutions. *Electrochimica Acta* 52(28): 7811–7819.

Lamaka, S. Zheludkevich, M. Yasakau, K. Montemor, M. and Ferreira, M. 2007. High effective organic corrosion inhibitors for 2024 aluminium alloy. *Electrochimica Acta* 52(25): 7231–7247.

Llopiz, P. and Maire, J. 1979. Infrared and ESCA studies of some metal-cysteine complexes. *Bulletin de la Societe Chimique de France* (11–12, Pt. 1): 457–62.

Loveday, D. Peterson, P. and Rodgers, B. 2004. Evaluation of organic coatings with electrochemical impedance spectroscopy, part 2: application of EIS to coatings. *JCT Coatings Tech* (October): 88–93.

MacLeod, I. and Wozniak, R. 1997. Corrosion and conservation of tin and pewter. . In *Metal 95: Proceeding of the International Conference on Metals Conservation*, ed. I. MacLeod et al. London: James and James. 118–23.

Madsen, H. B. 1967. A preliminary note on the use of benzotriazole for stabilizing bronze objects. *Studies in Conservation* 12(4): 163–167.

Madsen, H. B. 1971. Further remarks on the use of benzotriazole for stabilizing bronze objects. *Studies in Conservation* 16(3): 120–122.

Mansfeld, F. 2006. Electrochemical impedance spectroscopy. In *Analytical Methods in Corrosion Science and Engineering*, ed. P. Mrcus and F. Mansfeld. Taylor and Francis. 463–505.

Merk, L. E. 1981. The effectiveness of benzotriazole in the inhibition of the corrosive behaviour of stripping reagents on bronzes. *Studies in Conservation* 26(2): 73–76.

Mezzi, A. Angelini, E. De Caro, T. Grassini, S. Faraldi, F. Riccucci, C. and Ingo, G. M. 2012. Investigation of the benzotriazole inhibition mechanism of bronze disease. *Surface Interface Analysis*. 44(8): 968–971.

Molodkin, A. K. Vasilenko, T. G. Zaitsev, B. E. and Kuznetsov, S. L. 1997. Complex compounds of tin (II) and tin (IV) chlorides. *Russian Journal of Coordination Chemistry* 23(8): 543–549.

Organ, R. 1963. Aspect of bronze patina and its treatment. *Studies in Conservation*.8(1): 1–9.

Panigrahi, S. Kundu, S. Basu, S. Praharaj, S. Jana, S. Pande, S. Ghosh, S. Pal, A. and Pal, T. 2006. Cysteine functionalized copper organosol: synthesis, characterization, and catalytic application. *Nanotechnology* 17(21): 5461–5468.

Quraishi, M. Ansari, F. and Jamal, D. 2004. Corrosion inhibition of tin by some amino acids in citric acid solution. *Indian Journal of Chemical Technology* 11(2): 271–274.

Ramesh, V. Umasundari, P. and Das, K. 1998. Study of bonding characteristics of some new metal complexes of salicylaldoxime (SALO) and its derivatives by far infrared and UV spectroscopy. *Spectrochimica Acta Part A* 54(2): 285–297.

Rockland, L. 1960. Saturated salt solutions for static control of relative humidity between 5° and 40° C. *Analytical Chemistry* 32(10): 1375–1376.

Sarkar, M. 1991. Conductimetric determination of some metal ions using salicylaldoxime as the reagent. *Analyst* 116(5): 537–539.

Scott, D. A. 1990. Bronze Disease: A Review of Some Chemical Problems and the Role of Relative Humidity. *Journal of the American Institute for Conservation* 29(2): 193–206.

Sease, C. 1978. Benzotriazole: a review for conservator. *Studies in Conservation* 23(2): 76–85.

Sigma Aldrich MSDS 2013. http://www.sigmaaldrich.com/catalog/product/aldrich/190446?lang=en&region=JO.

Skerry, B. S. 1985. How corrosion inhibitors work. In *Corrosion Inhibitors in Conservation, Occasional Paper no. 4*, ed. S. Keene. London: The United Kingdom Institute for Conservation of Historic and Artistic Works. 5–12.

Strandberg, H. Johansson, L. and Lindqvist, O. 1997. The atmospheric corrosion of statue bronzes exposed to SO_2 and NO_2. *Materials and Corrosion* 48(11): 721–730.

Szymanowski, J. 1993. *Hydroxyoximes and copper hydrometallurgy*. Boca Raton: CRC press.

Zhang, D. Gao, L. and Zhou, G. 2005. Inhibition of copper corrosion in aerated hydrochloric acid solution by amino-acid compounds. *Journal of Applied Electrochemistry* 35(11): 1081–1085.

Sources of Materials
- High conductivity copper-110 and wrought phosphorous bronze-510:
AMAC Alloys, 38 Research Drive, Croydon South, Victoria 3136, Australia.
Phone: +61 3 9729 9222

- Salicylaldoxime ($C_7H_6O_2N$):
UNIVAR, 14 Williamson Rd, Ingleburn, NSW 2565, Australia.
Phone: +61 2 9618 1588

- Benzotriazole ($C_6H_5N_3$):
Merck Pty Limited, 207 Colchester Road, Kilsyth, Victoria 3137, Australia.
Phone: + 61 3 9728 7600